Mass measurements of neutron rich isotopes in the Fe region and electron capture processes in neutron star crusts

A. Estradé^{a,b,c*}, **M. Matoš**^{a,b†}, **H. Schatz**^{a,b,c}, **A. M. Amthor**^{a,b,c}, **D. Bazin**^{a}, **M. Beard**^{b,d}, **E. Brown**^{b,c}, **A. Becerril**^{a,b,c}, **T. Elliot**^{a,b,c}, **A. Gade**^{a,c}, **D. Galaviz**^{a,b‡}, **S. Gupta**^{e}, **W. R. Hix**^{f}, **R. Lau**^{a,b,c}, **G. Lorusso**^{a,b,c}, **P. Möller**^{e}, **J. Pereira**^{a,b}, **M. Portillo**^{a}, **A. M. Rogers**^{a,b,c§}, **D. Shapira**^{f}, **E. Smith**^{b,g}, **A. Stolz**^{a}, **M. Wallace**^{e}, **and M. Wiescher**^{b,d}.

^{a}*National Superconducting Cyclotron Laboratory, Michigan State University, USA*
^{b}*Joint Institute for Nuclear Astrophysics (JINA) , Michigan State University, USA*
^{c}*Department of Physics and Astronomy, Michigan State University, USA*
^{d}*Department of Physics, University of Notre Dame, USA*
^{e}*Los Alamos National Laboratory, USA*
^{f}*Physics Division, Oak Ridge National Laboratory, USA*
^{g}*The Ohio State University, USA*

E-mail: `a.estrade@gsi.de`

Experimental knowledge of nuclear masses of exotic nuclei is important for understanding nuclear structure far from the valley of β-stability, and as a direct input into astrophysical models. Electron capture processes in the crust of accreting neutron stars have been proposed as a heat source that can affect the thermal structure of the star. Nuclear masses of very neutron-rich nuclides are necessary inputs to model the electron capture process. The time-of-flight (TOF) mass measurement technique allows measurements on very short-lived nuclei. It has been effectively applied using the fast fragment beams produced at the National Superconducting Cyclotron Lab (NSCL) to reach masses very far from stability. Measurements were performed for neutron-rich isotopes in the region of the N=32 and N=40 subshells, which coincides with the mass range of carbon superburst ashes. We discuss reaction network calculations performed to investigate the impact of our new measurements and to compare the effect of using different global mass models in the calculations. It is observed that the process is sensitive to the differences in the odd-even mass staggering predicted by the mass models, and our new result for ^{66}Mn has a significant impact on the distribution of heat sources in the crust.

11th Symposium on Nuclei in the Cosmos
19-23 July 2010
Heidelberg, Germany.

---

*Current address: St. Mary's University, Canada, and GSI, Germany.
†Current address: Louisiana State University, USA.
‡Current address: Universidade de Lisboa, Portugal.
§Current address: Argonne National Laboratory, USA.

The neutron star crust is one astrophysical scenario where unstable isotopes play a significant role. It is the solid layer of ≈ 1 km thickness located beneath the thin atmosphere and ocean [1]. It is made of a lattice of neutron-rich nuclei embedded in a degenerate electron gas, and free neutrons in the inner crust. The density spans several orders of magnitude (10^6 g/cm^3 to 10^{13} g/cm^3). It represents a minor fraction of the neutron star mass, but is an important element to understand a variety of its processes and observations. This is the case in low mass X-ray binaries (LMXB) [2], where the neutron star accretes material from a close companion. LMXBs are some of the brightness sources in the X-ray sky, and have been extensively studied with modern X-ray satellites.

One open question about the neutron star crust is the characterization of its thermal profile. A few transiently accreting neutron stars have been observed going into periods of quiescence, when accretion is turned off (e. g. reference [3]). Cooling curves are then constructed by periodically observing the star's luminosity. It has been shown that the decay of the luminosity maps the temperature profile of the crust [4], thus providing a direct test of our understanding of the physics of the crusts, as well as related aspects of neutron star physics. For example, thermonuclear processes in the outer layers of the star (like the rp-process) affect the chemical composition of the crust, which is an important parameter to set its thermal conductivity. Ultimately, the late stages of the cooling curves reflect the temperature of the neutron star core, and provide a unique diagnostic probe to the unknown state of matter at extreme density conditions.

A detailed understanding of the thermal structure of the crust is also important to the question of carbon superbursts. These are a rare type of Type-I X-ray bursts that are orders of magnitude longer and more energetic than the regular bursts produced by the rp-process in neutron star's surface. A plausible explanation for superbursts is the ignition, in the outer layers of the crust, of carbon left over in the rp-process ashes [5]. The ignition depth has been derived from observations of the burst's light curves. However, the temperature required for carbon ignition at such depth (density) is too large compared to our best understanding of the crust thermal structure.

Non-equillibrium nuclear reactions in the crust of an accreting neutron star are a potential heat source that must be accounted for a quantitative understanding of its thermal profile [6]. As material is slowly pushed into the interior of the star by the accretion process, it reaches regions of increasing density and electron chemical potential (μ_e). These conditions make electron captures in the outer crust, and neutron emissions and pycnonuclear fusion reactions in the inner crust, energetically favorable. We restrict our study to processes in the outer crust, which involve isotopes within reach of mass measurements. The threshold for each electron capture is directly determined by the nuclear masses of the nuclei involved through the reaction Q-value: $Q_{EC}(A,Z) = M(A,Z) - M(A,Z-1)$. The reaction occurs at the depth where μ_e reaches this threshold. Thus, nuclear masses determine the crust depth where each transition takes place, and the details of its chemical composition. As recognized by Hansel and Zdunik [6], as a consequence of the odd-even staggering of nuclear binding energies, for reactions along an even A isobaric chain the magnitude of $Q_{EC}(A,Z)$ is in general larger for a capture on an even-even isotope than for the subsequent capture on the odd-odd daughter. The second reaction will immediately follow the capture into an even-even nucleus, and proceed in a non-equilibrium way releasing a fraction of Q_{EC} as thermal energy (the rest is radiated away by neutrinos). Therefore, nuclear masses also determine the amount of heating. In some instances, electron captures proceed through excited states in the daughter nuclide, increasing the electron capture threshold and reducing the fraction of energy radiated as neutrinos [7].
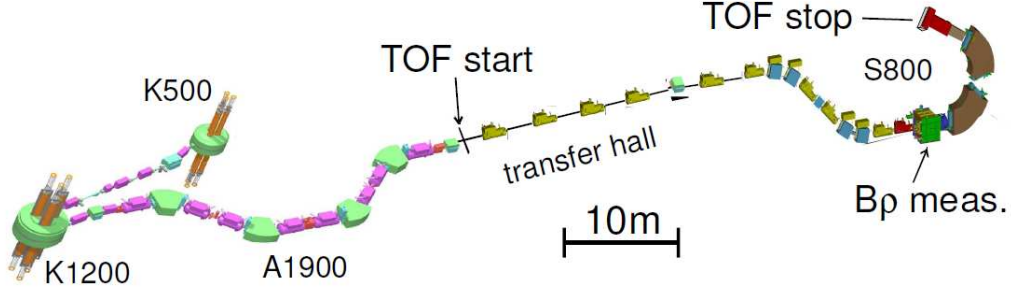
Figure 1: Experimental setup for TOF-Bρ mass measurements at the NSCL. The time-of-flight was measured with timing scintillators located at the exit of the A1900 fragment separator (TOF start) and at the S800 spectrometer focal plane (TOF stop), with a flight path of 58 m. The momentum was measured with MCP detectors located at the S800 dispersive plane (Bρ measurement). Be production targets were placed at the entrance of the A1900. The details of the setup are described in reference [9].

We measured the mass of 14 neutron-rich isotopes in the iron region, 4 of which were determined for the first time (^{61}V, ^{63}Cr, ^{66}Mn, and ^{74}Ni). The experiment was performed at S800 spectrometer beamline [8] of the National Superconducting Cyclotron Laboratory (NSCL) using the time-of-flight (TOF) technique [9] (Figure 1). TOF mass measurements are suitable to access the mass of very unstable isotopes due to the sensitivity of the method (beam rates as low as 0.01 particles per second) and the possibility of measuring several masses simultaneously [10]. The mass is derived from a simultaneous measurement of the TOF and the momentum of the beam particles. A radioactive ion beam was produced by fragmentation of a $100\,\mathrm{MeV/u}$ ^{86}Kr primary beam in Be production targets. By alternating targets of different thickness we included isotopes with well known masses in the secondary beam, which were used to calibrate the experimental setup. We used fast timing scintillators for the TOF measurement, and position sensitive micro-channel plate (MCP) detectors at the dispersive plane of the S800 spectrometer to measure the momentum. The setup provided a relative mass resolution of 1.8×10^{-4}. We estimated a systematic error of ≈ 100 keV (for $Z = 25$) from the normalization of the fit χ^2 results. The electron capture Q-values calculated with our measurement are shown in Figure 2. Detailed results will be presented in an upcoming publication.

We studied the impact of our results on crustal processes at accreting neutron stars with reaction network calculations following the approach of Gupta et al. [7]. The steady state composition of the crust is calculated by integrating the reaction network along the temperature profile of the star [11]. The energy released by each reaction is obtained from the difference of nuclear ground state energy between parent and daughter nuclei, and the change in the energy of the degenerate electron gas. The neutrino losses are calculated explicitly. For the composition of the outer layer of the crust we used the calculation of carbon superburst ashes from Schatz et al. [12], which includes isotopes in the mass range $40 \leq A \leq 68$. Because this is slightly neutron-rich material, the electron capture reactions will not take place until a depth corresponding to $\mu_e = 4$ MeV. The network was followed until a depth near the border of the outer and inner crust ($\mu_e = 16.5$ MeV).

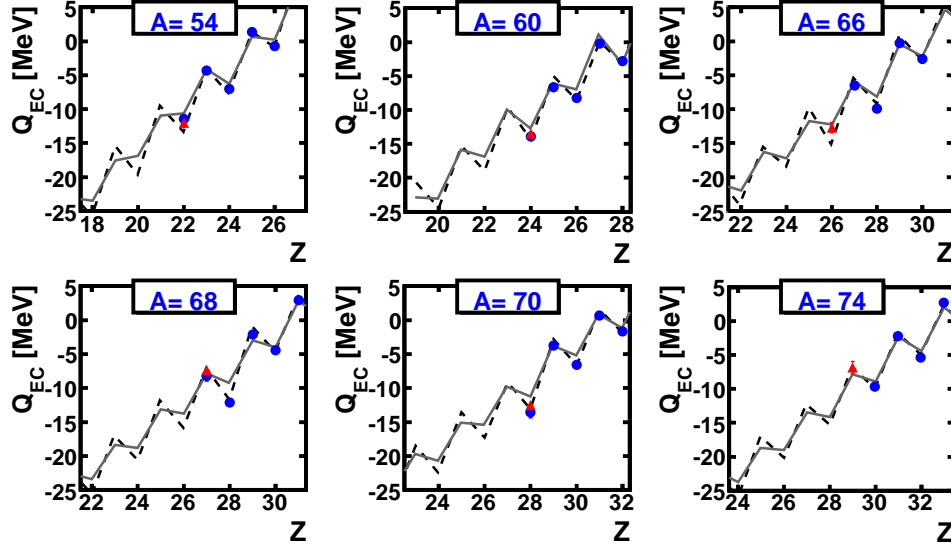We performed the calculations with two mass models commonly used for astrophysical appli-

Figure 2: Electron capture Q-values for even A isobaric chains determined with experimentally known masses and theoretical mass models ($Q_{EC}(A,Z) = M(A,Z) - M(A,Z-1)$). Red triangles correspond to Q-values obtained with the nuclear masses measured in our experiment, and blue circles to values calculated with literature masses [15]. In addition, the solid grey line shows results with masses from the HFB-14 model [14], and the dashed black line from the FRDM model [13]. The latter predicts a larger odd-even staggering in this region than HFB-14: Q_{EC} is more negative for the even-even nuclei, and less so for the odd-odd ones.

cations (FRDM [13], HFB-14 [14]), as well as experimentally known masses. Results are shown in Figure 3. The lower degree of odd-even mass stagering in this region predicted by the HFB-14 model compared to the FRDM model (Figure 2) is observed as a flatter energy deposition profile. In the HFB-14 case more reactions happen at threshold, and release less thermal energy in the crust. As a result, the integral of energy deposited in the outer crust is 20 % smaller. The results highlight the importance of constraining the odd-even staggering predicted by the mass models towards the neutron-rich isotopes.

Figure 3 also shows the results of simulations with Q-values calculated with experimentally known masses (complemented with the FRDM table). Two transitions are the main contribution to the crustal heating. These are the two-step electron captures ^{66}Ni $\rightarrow$ ^{66}Co $\rightarrow$ ^{66}Fe at a crust depth corresponding to $\mu_e \approx 9.3$ MeV, which proceeds through an excited state of ^{66}Fe, and ^{66}Fe $\rightarrow$ ^{66}Mn $\rightarrow$ ^{66}Cr at $\mu_e \approx 15$ MeV going through an excited state in ^{66}Cr. The calculation with masses from the literature does not include an experimental Q_{EC} value for ^{66}Fe, so that transition takes place as predicted by the FRDM model. Our first measurement of the ^{66}Mn mass leads to a threshold for the electron capture on ^{66}Fe that is 2.5 MeV smaller than the FRDM prediction. Therefore, this electron capture occurs at a significantly shallower depth, providing more efficient heating of the region where superbursts are ignited.

For a quantitative assessment of the consequences of our mass measurement for superburst ignition, reaction network calculations should be iterated with calculations of the star's thermodynamic profile. This will be done as a next step. Our new results put on a stronger experimental
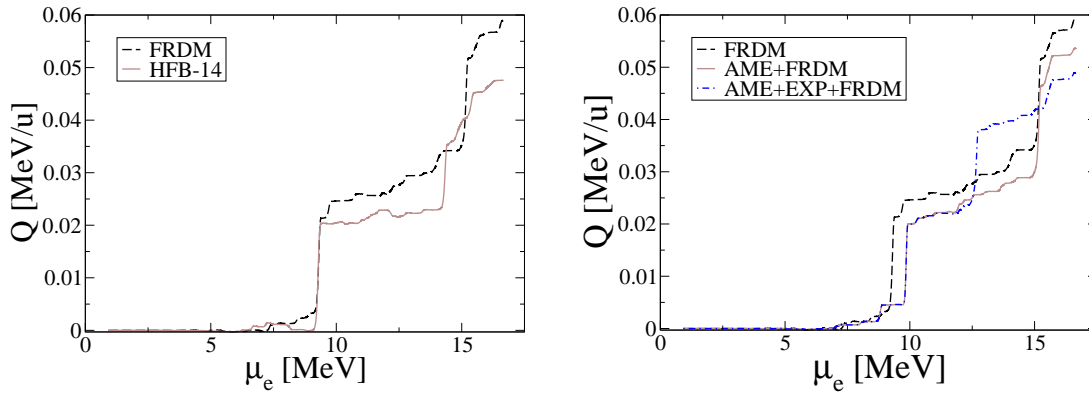
Figure 3: Thermal energy released by electron captures in the outer crust for an initial composition of superburst ashes. The curves show the thermal energy integral Q (in MeV per accreted nucleon) as a function of depth in the crust (expressed as the electron's chemical potential μ_e). The left plot shows results of calculations with nuclear masses from the FRDM and the HFB-14 models. The right plot shows calculations with experimental masses from the literature [15] (*AME+FRDM*), and including results of this experiment (*AME+EXP+FRDM*). The tables are complemented with the FRDM model (when the parent or daughter mass is not experimentally known only FRDM masses were used to calculate electron capture Q-values).

footing the calculations of nuclear processes in the outer crust for the mass region corresponding to the ashes of carbon superbursts. In addition, the reaction network calculations with different mass models show the importance of having reliable models extending out to the neutron dripline.

References

[1] J.M. Lattimer and M. Prakash, *Science*, (304), 536 (2004). `arXiv:astro-ph/0405262`

[2] T. M. Tauris and E. van den Heuvel, in *Compact stellar X-ray sources*, eds W. Lewin and M. van der Klis, Cambridge Astrophysics Series **39**, Cambridge, (2006). `arXiv:astro-ph/0303456`

[3] E. M. Cackett, et al., *Mon. Not. Roy. Astron. Soc.* **372**, 479 (2006). `arXiv:astro-ph/0605490`

[4] E. Brown, and A. Cumming *ApJ* **698**, 1020 (2009). `arXiv:astro-ph/0901.3115`

[5] A. Cumming and L. Bildsten, *ApJ* **559**, L127 (2001). `arXiv:astro-ph/0107213`

[6] P. Haensel and J. L. Zdunik, *A & A* **480**, 459 (2008). `arXiv:astro-ph/0708.3996`

[7] S. Gupta, et al., *ApJ* **662**, 1188 (2007). `arXiv:astro-ph/0609828`

[8] D. Bazin et al., *Nucl. Instr. and Meth.* **B204**, 629 (2003).

[9] M. Matoš, et al., *Jour. of Phys.* **G35**, 014045 (2008). `arXiv:astro-ph/0707.0119`

[10] H. Savajols, *Hyperfine Interactions* **132**, 245 (2001).

[11] E. Brown, *ApJ* **614**, L57 (2004). `arXiv:astro-ph/0409032`

[12] H. Schatz, et al., *Nucl. Phys.* **A718**, 247 (2003).

[13] P. Möller, et al., *At. Data Nucl. Data Tables* **59**, 185 (1995).

[14] S. Goriely, M. Samyn, and J.M. Pearson, *Phys. Rev.* **C75**, 064312 (2007).

[15] G. Audi, A. H. Wapstra, and C. Thibault, *Nucl. Phys.* **A729**, 337 (2003).